Structure of Confined Yukawa System (Dusty Plasma)

Hiroo Totsuji,* Tokunari Kishimoto, and Chieko Totsuji
Department of Electrical and Electronic Engineering, Okayama University, Tsushimanaka 3-1-1, Okayama 700, Japan
(Received 18 November 1996)

As a model of dusty plasmas, the structure of a Yukawa system confined in a one-dimensional external field is analyzed by molecular dynamics simulations and theoretical approaches. Particles form clear thin layers at low temperatures and the structure changes discretely with system parameters. The number and positions of layers and other characteristics are obtained as functions of dimensionless parameters. A simple sheet (shell) model with intralayer cohesive energy is shown to reproduce results of numerical experiments to a good accuracy. [S0031-9007(97)02964-5]

PACS numbers: 52.25.Wz, 52.65.−y

Dusty plasmas have recently been attracting much interest from the viewpoints of both basic plasma physics and plasma applications. The formation of dust crystals may be a typical example of interesting behaviors of dusty plasmas [1–4], and such dusty systems may serve as one of the ideal materials for experiments on classical fluids and solids [5]. In this Letter, we describe some results of numerical experiments on a dusty plasma [6] and present a simple and successful theoretical model.

The interaction potential between macroscopic dust particles depends on their own physical parameters and those of surrounding plasmas. There may exist various possibilities for these parameters and accordingly for the interaction potential. In order to understand the behavior of dusty plasmas in complicated situations, however, the results for simple and basic cases are indispensable. As one of those cases, we assume that macroscopic particles are interacting via the isotropic Yukawa (Debye-Hückel) potential [7]

$$v(r) = \frac{q^2}{r} \exp(-\kappa r) . \tag{1}$$

Here q is the charge (the same for all particles), r the distance, and $1/\kappa$ the screening length.

It has been shown [8–11] that the ion flow around a particle induces a wake field which can be viewed as composed of (1) [12] and an oscillating anisotropic part and the latter can align particles vertically. Being dependent on the Mach number, the anisotropic part may vary according to experimental apparatus and conditions, and there are also cases where one observes bcc and fcc (and hcp) structures without direct alignments [2]. We may have situations where the layered structure is mainly determined by the isotropic part, and the correlation of particle distribution in adjacent layers is determined by the anisotropic part. The Yukawa system seems to be still serving as a reference frame for experiments [5,13] and its analysis also clarifies the role of the anisotropic part by identifying what kinds of structures can or cannot result from (1).

In addition to mutual interactions, dust particles are under the effect of various external forces such as gravitation, electrostatic force, ion drug, and so on. We assume that the total effect of external forces is expressed by a simple one-dimensional confining potential

$$v_{\text{ext}}(z) = \frac{k}{2} z^2. \tag{2}$$

The uniformity in the xy plane may be satisfied around the center of the experimental apparatus. When the external forces, for example, the gravitation and the electrostatic force, balance with each other in the plane $z = 0$, we may simulate the total external potential near $z = 0$ by the parabolic form in the first approximation [14]. The uniform Yukawa system has long been extensively studied and its phase diagram and other statistical properties have already been analyzed [15]. We show structures and transitions between structures of the confined finite Yukawa system at low temperatures.

The classical Yukawa system in thermal equilibrium at the temperature T is characterized by two independent dimensionless parameters. With appropriately defined mean distance a, these parameters may be given by

$$\Gamma = \frac{q^2}{ak_BT} \quad \text{and} \quad \xi = \kappa a . \tag{3}$$

In the external field (2), we have another independent dimensionless parameter related to the ratio of the external potential to thermal energy ka^2/k_BT. Since our system is confined by a force along the z direction, the mean distance may be defined by $N_s = 1/\pi a^2$, where N_s is the surface number density in the xy plane.

In what follows, we are mainly concerned with the structure at low temperatures. Since both Γ and ka^2/k_BT diverge in this case, we adopt ξ and the ratio

$$\eta = \frac{\pi^{1/2}}{4} \frac{ka^2/k_BT}{q^2/ak_BT} = \frac{k}{4\pi q^2 N_S^{3/2}} \tag{4}$$

as two independent parameters. The extra factor is added for the sake of consistency with previous works with $\kappa = 0$ or the one-component plasma (OCP) [16,17].

In order to simulate the Yukawa system with infinite extensions in the xy plane, we impose the periodic boundary conditions. Since the shape of the periodicity sometimes

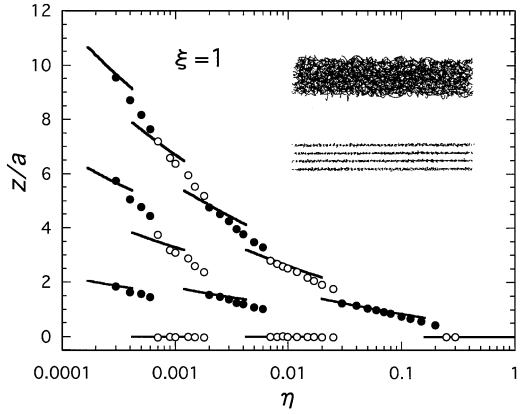

FIG. 1. Positions of layers for $\xi = 1$. Results of simulation (circles) and theory (lines). (Positions are symmetrical with respect to $z = 0$.) Inset: Orbits for $\eta = 0.002$ at high ($\Gamma = 100$, top) and low ($\Gamma = 3000$, bottom) temperatures.

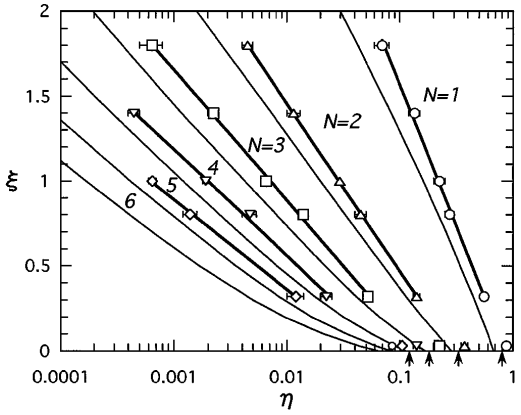

FIG. 2. Domains of $\mathcal{N}(= 1, 2, \ldots)$ layer structure. Symbols are boundaries determined by simulations for $\xi = 1.8$, 1.4, 1.0, 0.804, 0.322, and 0.0322 and thick lines are fittings of the form $\eta_c = \alpha \exp(-\beta\xi)$. (The small circle is the boundary of 6 and 7 for $\xi = 0.0322$.) Thin lines are boundaries given by our theory. Arrows are the first four boundaries for $\xi = 0$ in Ref. [22].

strongly influences the distribution, especially its symmetry, of particles, we take into account the deformation of fundamental vectors of periodicity as in the case of OCP [18] following Ref. [19], keeping the area of the unit cell in the xy plane constant [18]. We also introduce a virtual time and follow the dynamics of a virtual system to simulate the canonical ensemble [20].

Molecular dynamics simulations have been performed mainly with 1024 independent particles. Starting from states at sufficiently high T where particles form a cloud around $z = 0$, we slowly reduce T. With the decrease of T, microscopic structures appear in the cloud. At sufficiently low temperatures, particles organize themselves into well-defined thin layers as shown in the inset of Fig. 1, which plots the positions of layers as a function of η in the case of $\xi = 1$. The number of layers at low temperatures $\mathcal{N}$ depends on ξ and η; $\mathcal{N} = \mathcal{N}(\xi, \eta)$. In Fig. 2, we show boundaries of domains of the parameters where we have the states of $\mathcal{N}$ layers with $\mathcal{N} = 1, 2, \ldots$. In Fig. 3, we plot the total thickness of our system along z for several values of ξ.

The external potential $v_{\text{ext}}(z)$ tries to confine particles in the plane $z = 0$. In the limit of strong confinement or $\eta \gg 1$, particles are thus forced to be in the plane $z = 0$ and $\mathcal{N}(\xi, \eta) = 1$. Mutual repulsions between particles, on the other hand, tend to increase the thickness of particle distribution and the thickness increases when η becomes smaller. We here note that this tendency manifests itself as the appearance of a new layer with a finite population, analogously to the behavior of the order parameter in the first order phase transitions. In Figs. 1 and 3, we also observe that, when η decreases, the thickness increases with discontinuities corresponding to the stepwise changes in $\mathcal{N}$. The number of layers and the thickness are thus determined as a result of the competition between the confining force and mutual repulsion.

In the case of OCP, it has been shown that a confined finite system forms thin layers in accordance with the geometry of confinement at low enough temperatures and the number of layers and the total thickness change discretely with the system parameter [16,17,21,22]. Our results for the Yukawa system indicate that these properties are common for Coulomb and Coulomb-like systems.

In OCP, the spacings and populations for all layers are almost equal and the spacings increase with the decrease of η [17,21]. In our Yukawa system just after the appearance of a new layer, populations are nearly equal and outer layers have larger spacings (typically by 10%). With further decrease of η, outer layers become less populated (by 10% to 20%) and relative differences in spacings become smaller, all the spacings being expanded. Their values return to the initial state when another new layer appears and similar changes are repeated.

The critical values of η for the transition $\mathcal{N} \to \mathcal{N} + 1$, $\eta_c(\mathcal{N})$, is a function of ξ. In Fig. 2, we observe that $\eta_c(\mathcal{N}) \sim \alpha(\mathcal{N}) \exp[-\beta(\mathcal{N})\xi]$ for $\xi \gtrsim 0.3$. Values of

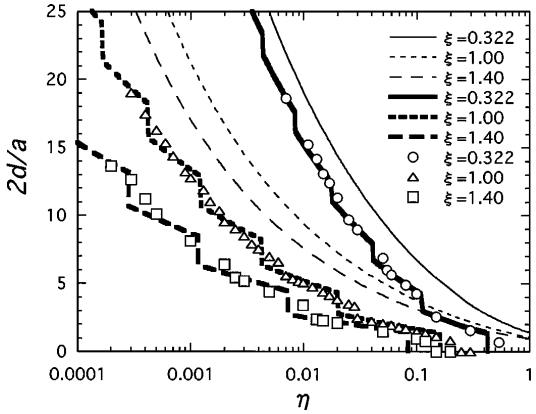

FIG. 3. Total thickness. Symbols are results of simulations. Thin and thick lines are those of the continuum model (6) and sheet model with cohesive energy (8), respectively.

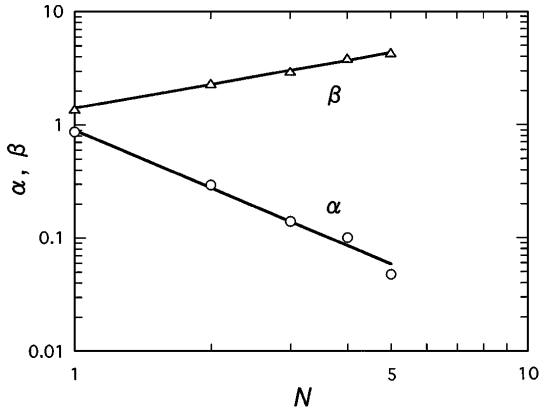

FIG. 4. Behavior of coefficients $\alpha(\mathcal{N})$ and $\beta(\mathcal{N})$. Solid lines are $0.9\mathcal{N}^{-1.7}$ and $1.4\mathcal{N}^{0.7}$, respectively.

α and β are approximately given by $\alpha(\mathcal{N}) \sim 0.9\mathcal{N}^{-1.7}$ and $\beta(\mathcal{N}) \sim 1.4\mathcal{N}^{0.7}$, respectively, as shown in Fig. 4. Since all layers have approximately equal populations, the mean distance in the layer is approximately given by $b = \mathcal{N}^{1/2}a$. Therefore the ratio of the mutual repulsion and confining force at b is given by

$$\frac{kb^2}{(q^2/b)\exp(-\kappa b)} = 4\pi^{-1/2}\mathcal{N}^{3/2}\eta\exp(\mathcal{N}^{1/2}\xi). \quad (5)$$

If the transitions occur when this ratio reaches a certain value, we may have $\alpha(\mathcal{N}) \propto \mathcal{N}^{-3/2}$ and $\beta(\mathcal{N}) \propto \mathcal{N}^{1/2}$. Experimental behavior of η_c indicates that this picture works as a first estimation.

Along with the decrease of η in the range between the appearance of a new layer and that of another new layer, the symmetry of distribution of particles in each layer repeats alternative changes from that of the square lattice to the triangular lattice. The relation between the interlayer distance and intralayer symmetry is shown in Fig. 5. This kind of transition may be analogous to the case of OCP [22] and colloidal suspensions confined between glass plates [23], where systematic changes of the symmetry with an increase or decrease of the number of layers have been observed. Three-dimensionally, structures similar to bcc, fcc, and hcp lattices appear in our system. Correspondence with characteristic parameters, however, is not yet completely clear. It seems that structures with vertical alignments between adjacent layers do not appear. This may indicate the role of anisotropic interaction in vertical alignments in real experiments.

We now make theoretical analyses along the lines of the shell model which have been successful for OCP [16,17]. Starting from the continuum model, we take into account the discreteness in two steps.

In the one-dimensional potential field $v_{\rm ext}(z)$, the total potential energy (per particle) of the uniform distribution with thickness $2d$ is given by

$$\frac{1}{6}kd^2 + \frac{\pi}{2}\frac{q^2N_s}{\kappa^3d^2}[\exp(-2\kappa d) - 1 + 2\kappa d]. \quad (6)$$

One might expect that the thickness of our system is estimated by the value of $2d$ which minimizes this expression. In Fig. 3, optimum values of $2d/a$ are shown by thin lines. When $\xi \ll 1$, our results for $2d/a$ are in good agreement with those of numerical experiments. For finite values of ξ, however, this model largely overestimates $2d/a$. In (6), particles are treated as continuum and the effects of discreteness or the correlation between particle positions are completely neglected. The above result indicates that we have to take them into account.

The effects of discreteness appear as (i) the formation of layers perpendicular to the z axis and (ii) the formation of lattice structures in each layer. Let us first assume that our system is composed of thin planar sheets and take (i) into account. Suppose we have $\mathcal{N}$ thin planar sheets of surface number densities n_i at $z = z_i$, $i = 1, 2, \ldots \mathcal{N}$, and $N_s = \sum_i n_i$. When particles are distributed uniformly in each layer, the total potential energy per particle is given by

$$\frac{1}{2}\sum_i \frac{n_i}{N_s}kz_i^2 + \frac{\pi}{N_s}\frac{q^2}{\kappa}\sum_{ij} n_i n_j \exp(-\kappa|z_i - z_j|). \quad (7)$$

When we minimize (7) with respect to n_i and z_i for given values of N_s and k, experimental thickness is approximately reproduced, if $\mathcal{N}$ is appropriately assumed. The

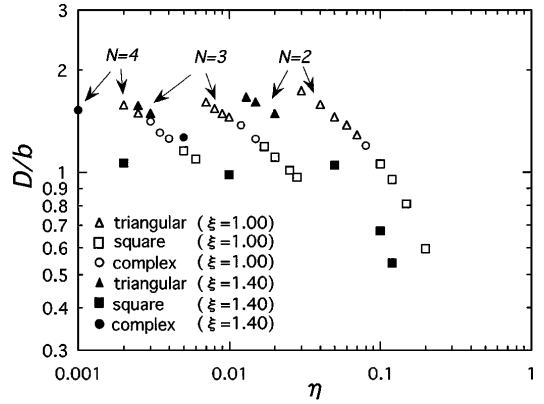

FIG. 5. Intralayer symmetry and interlayer spacing D, b being mean distance in layer.

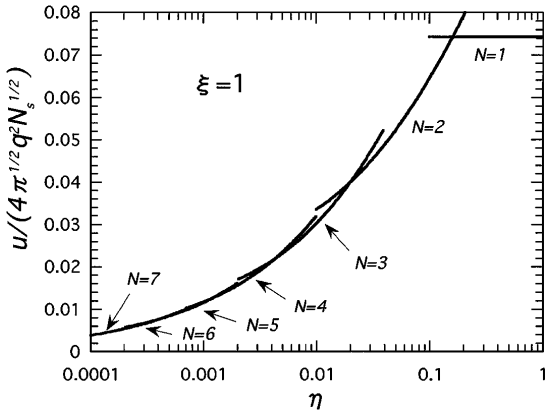

FIG. 6. Total energy u in sheet model with cohesive energy.

global minimum, however, is given by the state of infinite sheets ($\mathcal{N} \to \infty$) as in the case of OCP [16].

In order to include (ii), we define the cohesive energy as the difference between the interaction energy with correlation and that of uniform distribution. Since the effect of discreteness in the xy plane leads to a negative cohesive energy in each sheet, we have a possibility to stabilize the state of finite number of sheets: There is a tradeoff between intersheet interaction energy and intrasheet cohesive energy which is lower for larger density in each sheet and favors smaller number of sheets. The cohesive energy per particle for a sheet of the surface density n_i is expressed by a function of $\kappa n_i^{-1/2}$ as $q^2 n_i^{1/2} e_{\rm coh}(\kappa n_i^{-1/2})$. We have calculated values of $e_{\rm coh}(x)$ for the triangular and square lattices.

The total potential energy is thus given by

$$\frac{1}{2}\sum_i \frac{n_i}{N_s} k z_i^2 + \frac{\pi}{N_s}\frac{q^2}{\kappa}\sum_{ij} n_i n_j \exp(-\kappa|z_i - z_j|) + \sum_i \frac{n_i}{N_s} q^2 n_i^{1/2} e_{\rm coh}(\kappa n_i^{-1/2}) . \quad (8)$$

When we minimize (8) with respect to all parameters for given N_s and k, we have the results which reproduce the transitions between structures. An example is shown in Fig. 6. The results for positions, critical values of transitions, and thickness are given by solid lines in Figs. 1, 2, and 3. Values of $e_{\rm coh}(\kappa n_i^{-1/2})$ for both triangular and square lattices give almost the same results. Though values of η_c are somewhat small, our simple model successfully reproduces the main features of structure of Yukawa system in external fields at low temperatures.

The effect of discreteness also appears as interlayer correlation in the distributions of particles neglected in (8). This effect is closely connected with the alternate changes in the intralayer symmetries shown in Fig. 5 and may also be related to systematic deviations of η_c from simulations. We may conclude, however, the overall behavior of the confined Yukawa system is reproduced by our sheet (shell) model with intralayer cohesive energy.

We have shown that the confined Yukawa system organizes itself into layered structures at low temperatures and its behavior is approximately reproduced by a simple model. In the latter, the inclusion of the cohesive energy in the layer is of essential importance to give transitions between structures.

This work is partly supported by Grants-in-Aid for Scientific Research from the Ministry of Education, Science, Sports, and Culture of Japan, No. 06680448 and No. 08458109.

*Electronic address: totsuji@mat.elec.okayama-u.ac.jp

[1] H. Thomas, G. E. Morfill, V. Demmel, J. Goree, B. Feuerbacher, and D. Möhlmann, Phys. Rev. Lett. **73**, 652 (1994).
[2] J. H. Chu and Lin I, Physica (Amsterdam) **205A**, 183 (1994); Phys. Rev. Lett. **72**, 4009 (1994).
[3] Y. Hayashi and K. Tachibana, Jpn. J. Appl. Phys. **33**, L804 (1994).
[4] A. Melzer, T. Trottenberg, and A. Piel, Phys. Lett. A **191**, 301 (1994).
[5] For example, H. M. Thomas and G. E. Morfill, Nature (London) **379**, 806 (1996).
[6] Some earlier results have been given in H. Totsuji, T. Kishimoto, Y. Inoue, C. Totsuji, and S. Nara, Phys. Lett. A **221**, 215 (1996).
[7] H. Ikezi, Phys. Fluids **29**, 1764 (1986).
[8] S. V. Vladimirov and M. Nambu, Phys. Rev. E **52**, 2172 (1995).
[9] F. Melandsø and J. Goree, Phys. Rev. E **52**, 5312 (1995).
[10] S. V. Vladimirov and O. Ishihara, Phys. Plasmas **3**, 444 (1996); O. Ishihara and S. V. Vladimirov, Phys. Plasmas **4**, 69 (1997).
[11] A. Melzer, V. A. Schweigert, I. V. Schweigert, A. Homann, S. Peters, and A. Piel, Phys. Rev. E **54**, R46 (1996); V. A. Schweigert, I. V. Schweigert, A. Melzer, A. Homann, and A. Piel, Phys. Rev. E **54**, 4155 (1996).
[12] We have the Debye-Hückel screening also in nonneutral plasmas as shown in R. C. Davidson, *Physics of Nonneutral Plasmas* (Addison-Wesley Publishing Company, Redwood City, California, 1990), Chap. 3.
[13] A. Melzer, A. Homann, and A. Piel, Phys. Rev. E **53**, 2757 (1996).
[14] This similarity to the one-component plasma confined in a parabolic potential has been pointed out in Ref. [13].
[15] For example, M. O. Robbins, K. Kremer, and G. S. Grest, J. Chem. Phys. **88**, 3286 (1988); S. Hamaguchi and R. T. Farouki, J. Chem. Phys. **101**, 9876 (1994); **101**, 9885 (1994).
[16] H. Totsuji and J.-L. Barrat, Phys. Rev. Lett. **60**, 2484 (1988).
[17] H. Totsuji, *Strongly Coupled Plasma Physics*, edited by S. Ichimaru (Elsevier Science Publishers, New York, 1990), p. 213; Phys. Rev. E **47**, 3784 (1993).
[18] H. Totsuji, H. Shirokoshi, and S. Nara, Phys. Lett. A **162**, 174 (1992).
[19] M. Parrinello and A. Rahman, Phys. Rev. Lett. **45**, 1196 (1980); M. Parrinello, A. Rahman, and P. Vashishta, Phys. Rev. Lett. **50**, 1073 (1983).
[20] S. Nosé, J. Chem. Phys. **81**, 511 (1984); H. C. Andersen, J. Chem. Phys. **72**, 2384 (1980).
[21] J. P. Schiffer, Phys. Rev. Lett. **61**, 1843 (1988); **70**, 818 (1993).
[22] D. H. E. Dubin, Phys. Rev. Lett. **71**, 2753 (1993).
[23] D. H. Van Winkle and C. A. Murray, Phys. Rev. A **34**, 562 (1986).